Parton-hadron matter at finite temperature and chemical potential



2015 J. Phys.: Conf. Ser. 636 012016

(http://iopscience.iop.org/1742-6596/636/1/012016)

Journal of Physics: Conference Series **636** (2015) 012016 doi:10.1088/1742-6596/636/1/012016

# Parton-hadron matter at finite temperature and chemical potential

**E L Bratkovskaya[1], V P Konchakovski[2], W Cassing[2]**

[1] Institute for Theoretical Physics, University of Frankfurt, Frankfurt, Germany
[2] Institute for Theoretical Physics, University of Giessen, Giessen, Germany
[3] Texas A& M Universtity, Texas,U.S.A.

E-mail: Elena.Bratkovskaya@th.physik.uni-frankfurt.de

**Abstract.** The dynamics of partons and hadrons in ultra-relativistic nucleus-nucleus collisions is analyzed within the Parton-Hadron-String Dynamics (PHSD) transport approach, which is based on a dynamical quasiparticle model for the partonic phase (DQPM) including a dynamical hadronization scheme while reproducing lattice QCD results in thermodynamic equilibrium for the equation-of-state as well as transport coefficients like shear and bulk viscosities or the electric conductivity of the hot QCD medium. The PHSD model reproduces a large variety of observables from SPS to LHC energies, e.g. the quark-number scaling of elliptic flow, transverse mass and rapidity spectra of charged hadrons, dilepton spectra, open and hidden charm production, collective flow coefficients etc., which are associated with the observation of a strongly interacting QGP (sQGP). The 'highlights' of the latest results from LHC energies are presented with a focus on the correlation between the average transverse momentum $< p_T >$ and the number of charged particles $N_{ch}$ in p-p, p-Pb and Pb-Pb collisions at midrapidity as observed by the ALICE Collaboration.

## 1. Introduction

The dynamics of the early universe in terms of the 'Big Bang' may be studied experimentally by ultra-relativistic nucleus-nucleus collisions at Relativistic-Heavy-Ion-Collider (RHIC) or Large-Hadron-Collider (LHC) energies in terms of 'tiny bangs' in the laboratory. With sufficiently strong parton interactions, the medium in the collision zone can be expected to achieve local equilibrium after some initial delay and exhibit approximately hydrodynamic flow [1, 2, 3]. In these collisions a new state of strongly interacting matter is created, being characterized by a very low shear viscosity $\eta$ to entropy density $s$ ratio, $\eta/s$, close to a nearly perfect fluid [4, 5]. Lattice QCD (lQCD) calculations [6, 7] indicate that a crossover region between hadron and quark-gluon matter should have been reached in these experiments.

In case of nuleus-nucleus (e.g. Pb+Pb) collisions the ideal or viscous hydro calculations the initial conditions – at some finite starting time of the order of 0.3 to 0.5 fm/c – have to be evaluated either in terms of the (standard) Glauber model or other initial state scenarios like the IP-glasma model [8, 9] or the CGC approach [10, 11, 12, 13], respectively. Alternative initial state scenarios are a coherent or incoherent superposition of 'strings' [14] or just an incoherent superposition of hard nucleon-nucleon collisions as in the wounded nucleon model (WNM) [15]. Differences between the different initial state assumptions and dynamical evolutions thus have to be expected. The applicability of ideal or viscous hydrodynamic models to proton-nucleus

reactions for low multiplicity events, however, is very much debated. This also holds for hybrid models [16, 17] as long as they employ a hydro phase. To our knowledge only microscopic transport approaches [18, 19] allow to bridge the gap from p-p to p-A and A-A collisions in a unique way without introducing additional (and less controlled) parameters. We will here employ the microscopic Parton-Hadron-String Dynamics (PHSD) transport approach [20] to analyze early reaction dynamics in the context of collective flow coefficients to shed some light on the sensitivity of these observables on different assumptions on the initial state dynamics.

The complexity of heavy-ion collisions is reduced essentially in the case of proton-nucleus collisions owing to the expected dominance of the initial state effects. In 2013 the first ALICE measurement of the charged particle pseudorapidity density has been reported [21] for $|\eta| < 2$ in p-Pb collisions at a nucleon-nucleon center-of-mass energy $\sqrt{s_{NN}} = 5.02$ TeV. The measurement has been compared to two sets of particle production models that describe similar measurements for other collision systems: the saturation models employing coherence effects [11, 12] and the two-component models combining perturbative QCD processes with soft interactions [22, 23]. A comparison of the model calculations with the data has shown that the results are model-dependent and predict the measured multiplicities only within 20%. Accordingly, the restrictions imposed by the measured minimal bias pseudo-rapidity spectra $dN_c/d\eta$ are not sufficient to disentangle different models for the very early interaction stage of ultra-relativistic collisions. We will here employ the PHSD approach to study p-Pb and Pb-Pb reactions on an event-by-event basis in order to obtain further information on correlations between different observables such as the correlation between the average transverse momentum $< p_T >$ and the number of charged particles $N_{ch}$ at midrapidity as observed by the ALICE Collaboration.

## 2. PHSD @ LHC

We briefly recall the ingredients of the PHSD which is a covariant dynamical approach for strongly interacting systems formulated on the basis of Kadanoff-Baym equations [24] or off-shell transport equations in phase-space representation, respectively. In the Kadanoff-Baym theory the field quanta are described in terms of dressed propagators with complex selfenergies. Whereas the real part of the selfenergies can be related to mean-field potentials (of Lorentz scalar, vector or tensor type), the imaginary parts provide information about the lifetime and/or reaction rates of time-like particles [25]. Once the proper (complex) selfenergies of the degrees-of-freedom are known, the time evolution of the system is fully governed by off-shell transport equations (as described in Refs. [24, 25]). The PHSD approach includes a dynamical hadronization scheme based on transition rates and incorporates elastic and inelastic interactions of hadrons in the final expansion stage as in the HSD model [26]. This approach allows for a simple and transparent interpretation of lattice QCD results for thermodynamic quantities as well as correlators in the partonic stage and leads to effective strongly interacting partonic quasiparticles with broad spectral functions. For a review on off-shell transport theory we refer the reader to Ref. [25]. Actual PHSD results and their comparison with experimental observables for heavy-ion collisions from the lower super-proton-synchrotron (SPS) to RHIC energies can be found in Refs. [20, 27, 28] including electromagnetic probes such as $e^+e^-$ or $\mu^+\mu^-$ pairs [29, 30].

### *2.1. p-p reactions at the LHC*

To extend the PHSD model to higher energies than $\sqrt{s_{NN}} = 200$ GeV at RHIC, we have additionally implemented the PYTHIA 6.4 generator [31] for initial nucleon collisions at LHC energies. For the subsequent (lower energy) collisions the standard PHSD model [20] is applied (including PYTHIA v5.5 with JETSET v7.3 for the production and fragmentation of jets [32], i.e. for $\sqrt{s_{NN}} \leq 500$ GeV [32]). In this way all results from PHSD up to top RHIC energies are regained and a proper extension to LHC energies is achieved. At $\sim \sqrt{s_{NN}} = 500$ GeV both PYTHIA versions lead to very similar results. In PYTHIA 6.4 we use the Innsbruck pp tune

(390) which allows to describe reasonably the p-p collisions at $\sqrt{s_{NN}} = 7$ TeV in the framework of the PHSD transport approach. The overall agreement with LHC experimental data for the distribution in the charged particle multiplicity $N_{ch}$ (a), the charged particle pseudorapidity distribution (b), the transverse momentum $p_T$ spectra (c) and the correlation of the average $p_T$ with the number of charged particles (d) is satisfactory (cf. Fig. 1).

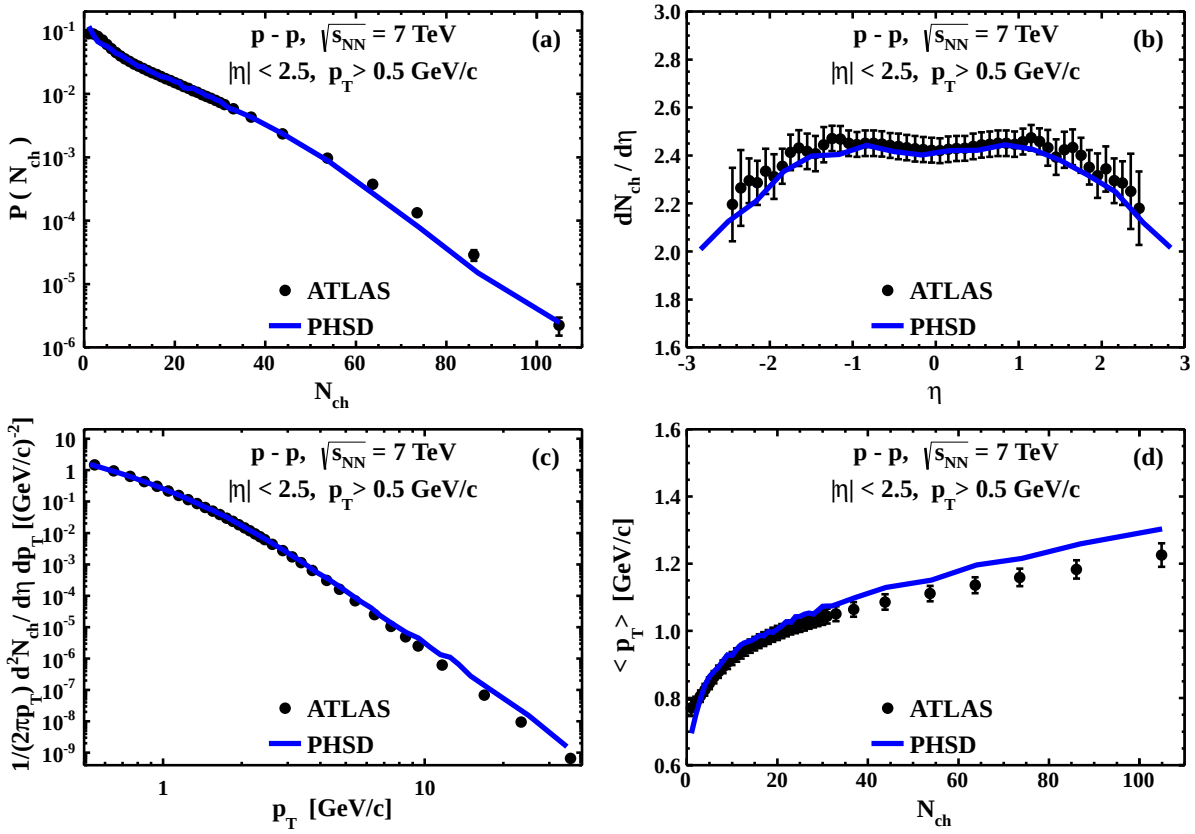


**Figure 1.** Comparison of the PHSD results (including PYTHIA 6.4) with LHC experimental data from the ATLAS Collaboration [33] for p-p collisions at $\sqrt{s_{NN}} = 7$ TeV: (a) $N_{ch}$ distribution, (b) $dN_{ch}/d\eta$ distribution, (c) $p_T$-spectra and (d) average $p_T$ vs. $N_{ch}$.

*2.2. Properties of p-Pb collisions at the LHC*

With the elementary p-p collisions in the PHSD being adjusted at LHC energies via PYTHIA 6.4 (using the Innsbruck pp tune (390)) we proceed with observables and correlations from p-Pb collisions. In Fig. 2 (lhs) we present the probability distribution in the participant number $N_{part}$ and the number of charged hadrons at midrapidity $N_{ch}(\eta = 0)$ as well as the ensemble average $< N_{ch} >$ vs. $N_{part}$ (rhs) for p-Pb ($\sqrt{s_{NN}}$=5.02 TeV). As is seen from Fig. 2 (lhs), the number of charged particles at midrapidity correlates with the number of participants, $N_{ch}(\eta = 0) \sim N_{part}$, however, with a large dispersion in both quantities. When considering the ensemble average $< N_{ch}/d\eta >$ $(\eta = 0)$ vs. $N_{part}$ we obtain the solid (blue) line within PHSD while the dotted (red) line results from PHSD when including additionally fluctuations in the cross section (PHSD GG). For details we refer the reader to Ref. [34]. Both the standard Glauber and CGC results are presented and support the results of Ref. [15]. The two versions of the PHSD model, with (red dotted line) and without cross section fluctuations (blue solid line), predict that the multiplicity dependence turns out to be close to the CGC result but substantially differs from the wounded

nucleon model (WNM) for larger $N_{part}$. Thus, multiplicity distributions do not allow us to disentangle the different initial states under discussion from the CGC and a Glauber version as in PHSD. The reason of such a multiplicity suppression relative to the WNM is the energy-momentum conservation in PHSD which on average results in a decrease of particle multiplicity in subsequent scatterings as compared to the primary interaction.

The pseudorapidty distributions of charged particles from p-Pb minimum bias collisions at $\sqrt{s_{NN}} = 5.02$ TeV are compared with the experimental data [21] in Fig. 3. The data are displayed in the laboratory system which is shifted with respect to the nucleon-nucleon center-of-mass by $y_{cm} = -0.465$. The results of two versions of the parton-hadron string dynamics model (PHSD and PHSD-GG) differ only for backward-emitted particles and both versions are rather close to the measured data and the CGC result (open circles). Note that there are no modifications (or free parameters) in the PHSD except the extensions by PYTHIA 6.4 which implies that p-p, p-A and A-A collisions are consistently described from low SPS to LHC energies (within $\sim 10\%$).

The CGC predictions from Ref. [13], performed earlier for the upcoming p-Pb run at the LHC, are plotted in the same figure (open circles). This result is based on the Balitsky-Kovchegov (BK) equation [35] which is the large-$N_c$ limit of non-linear renormalization group equations such as the BK-JIMWLK hierarchy [36] which is tested with respect to $e + p$ data. An astonishing result is that the CGC and PHSD results almost coincide again. Note that this minimum-bias distribution corresponds to the mean charged particle multiplicity at the given value of pseudorapidity $\eta$. However, event fluctuations of $dN_{ch}/d\eta$ are very large as demonstrated in Fig. 3 (rhs). Thus, the study of minimum-bias $dN_{ch}/d\eta$ does not allow to disentangle the initial state concepts described within the PHSD and CGC approaches.

Let us, furthermore, consider pseudorapidity distributions for fixed high-multiplicity events. Such distributions for different centrality bins have been measured by the ATLAS collaboration [37] for p-Pb collisions at $\sqrt{s_{NN}} = 5.02$ TeV. Experimentally the centrality was defined according to selected bins in the transverse energy. We have defined corresponding bins in $N_{ch}$ keeping the same percentage of the number of selected events as in [37] (the bin partition is shown in Fig. 4 (lhs) and the relative contribution of different centralities is given in the legend

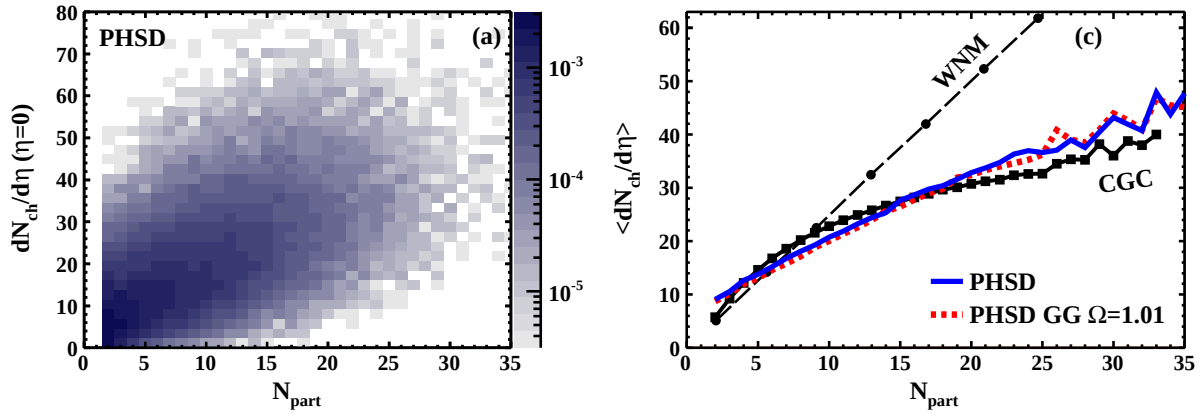


**Figure 2.** Probability distribution of the participant number and number of charged particles for Pb+Pb at $\sqrt{s_{NN}} = 5.02$ TeV at midrapidity (lhs) and its ensemle average in comparison to different models (rhs). The wounded nucleon model (WNM)(full dots) and color glass condensate (CGC) calculations (dotted line) are taken from Ref [15] while simulations in the Glauber-Gribov approximation (full squares and triangles) stem from Ref. [37]. The PHSD results are displayed in terms of the solid (blue) lines while the PHSD results including fluctuations in the cross section (PHSD GG) are shown in terms of the dotted (red) lines.

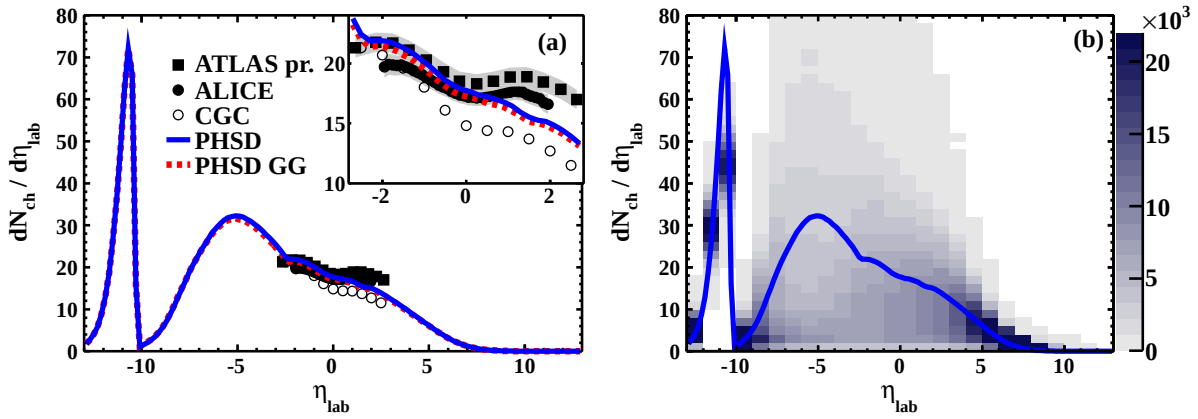


**Figure 3.** (lhs) Rapidity distribution of charged particles for minimum bias data from the ALICE [21] (full dots) and ATLAS [37] (full squares) collaborations for p-Pb collisions at $\sqrt{s_{NN}} = 5.02$ TeV in comparison to the PHSD results (solid blue line) and the PHSD GG results including fluctuations in the cross section (dotted red line). The CGC results (open circles) have been taken from Ref. [13]. The zoomed results are displayed in the insertion. (rhs) Event-by-event fluctuations of the rapidity distribution. The blue solid line shows the average charged particle pseudorapidity distribution.

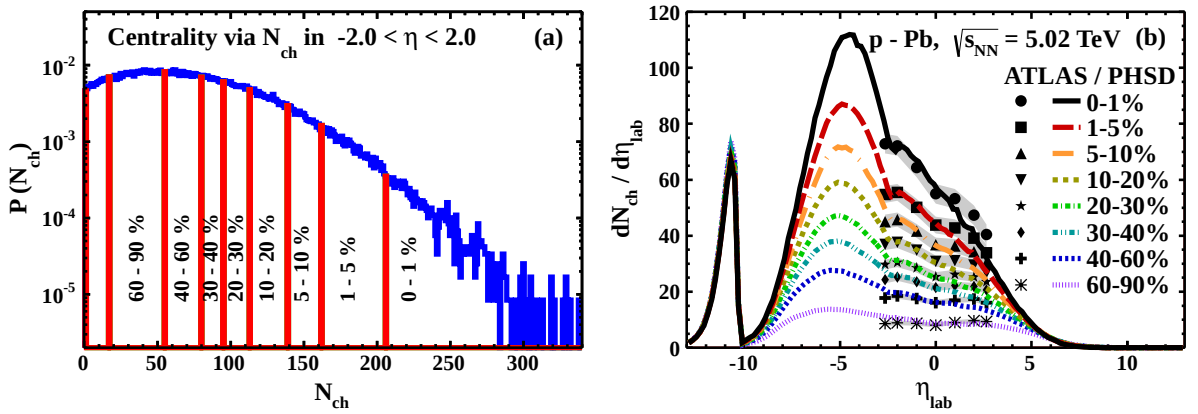


**Figure 4.** (lhs) Centrality bins for p-Pb collisions at $\sqrt{s_{NN}} = 5.02$ TeV selected according to the charged particle multiplicity in the rapidity interval $|\eta| < 2$. (rhs) Comparison of the PHSD calculated rapidity distributions with ATLAS data [37] for charged particles in different centrality bins. The shaded bands show the experimental uncertainties.

in Fig. 4 (rhs)). In this figure the PHSD results are based on $10^6$ simulated events.

As is seen from Fig. 4 (rhs), the PHSD model quite well reproduces the shape of the $dN_{ch}/d\eta$ distributions and its variation with centrality, in particular the increase with centrality of the forward-backward asymmetry between the directions of the proton-beam and Pb-target. For the most central events the PHSD calculations very slightly overshoot this asymmetry, however, are in line with the data for the higher centralities within the experimental uncertainties (shaded areas in Fig. 4 (rhs)). We mention that the centrality sample of 40-60% with the maximal number $N_{ch} \sim 20$ roughly corresponds to the minimum-bias distribution. For events of the highest multiplicity which amount to (0-1)% – corresponding to $\sim 6.10^3$ simulated events – the number of charged particles at the maximum of the distribution is about 75. The agreement

between calculations and data is not so bad taking into account the experimental error bands and the fact that PHSD has no free parameters once the p-p dynamics is fixed (by the PYTHIA tune).

### *2.3. Pb-Pb collisions at $\sqrt{s_{NN}}$=2.76 TeV*

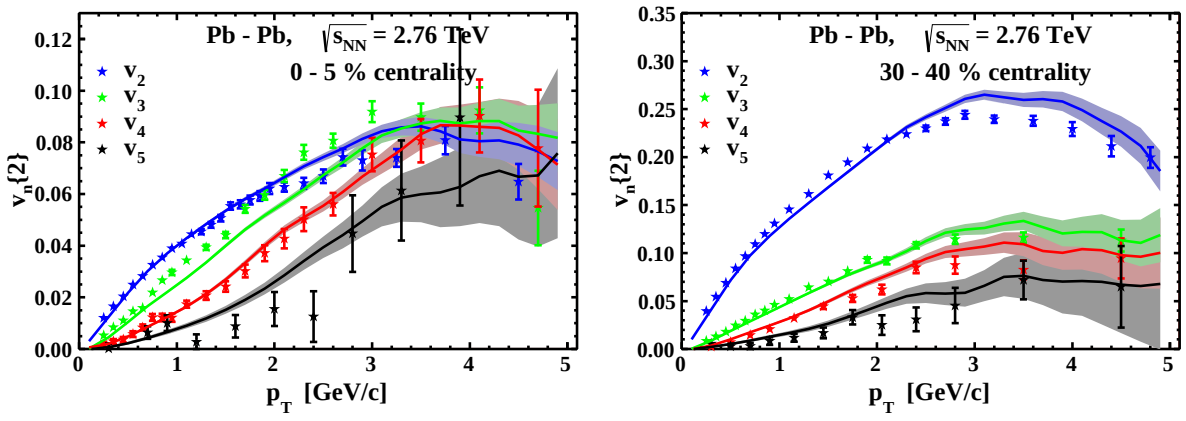


**Figure 5.** The flow coefficients $v_2$, $v_3$, $v_4$ and $v_5$ of all charged particles as a function of $p_T$ for the centralities 0-5% (lhs) and 30-40% (rhs). The ALICE data have been taken from Ref. [39].

Some general results for Pb-Pb collisions from the PHSD approach have been reported in Ref. [42]. Whereas the transverse charged single-particle spectra compare quite well with the experimental observations at the LHC [42] the question about the collective behavior of the system is of special interest. Anisotropic flow coefficients in both cases – i.e. experimental data and PHSD calculations – have been obtained from the two-particle cumulant method [43] in the central pseudorapidity window $|\eta| < 0.8$ and denoted as $v_n\{2\}$. In Fig. 5 we compare the flow coefficients $v_2$, $v_3$, $v_4$ and $v_5$ of all charged particles from PHSD as a function of $p_T$ for the centralities 0-5% (lhs) and 30-40% (rhs) in comparison to the ALICE data from Ref. [39]. The PHSD results for $v_2(p_T), v_3(p_T)$ and $v_4(p_T)$ compare reasonably up to about 3.5 GeV/c whereas at higher transverse momenta the statistics is insufficient to draw robust conclusions. This also holds for the flow coefficient $v_5$ which still is in line with the data within error bars. It is quite remarkable that the collective behavior is reproduced not only for semi-central collisions (rhs) but also for 0-5% central collisions (lhs) that are more sensitive to the initial fluctuations [17]. These tests indicate that the 'soft' physics at LHC in central A-A reactions is very similar to the top RHIC energy regime although the invariant energy is higher by more than an order of magnitude. Furthermore, the PHSD approach seems to work from lower SPS energies up to LHC energies for p-p, p-A as well as A-A collisions, i.e. over a range of more than two orders in $\sqrt{s_{NN}}$.

We note in passing that a detailed study of the sensitivity of the initial state fluctuations in space on the collective flow coefficients $v_2, v_3$ and $v_4$ turned out to be negative even for very central ($b$=0) Pb-Pb collisions at the LHC (cf. Ref. [42]) which is essentially due to the fact that the global shape characteristics do not change much when increasing the local fluctuations. Thus our studies do not support the suggestion that the collective flow coefficients might be used to discriminate CGC from Glauber initial state conditions.

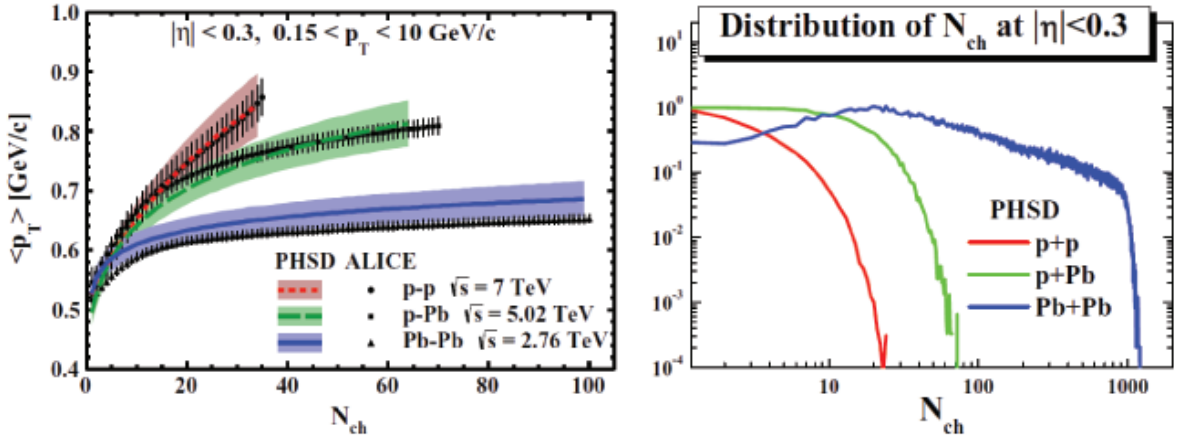


**Figure 6.** (lhs) Average $p_T$ results for p-p, p-Pb and Pb-Pb collisions from the PHSD transport approach [42] in comparison to the ALICE experimental data from Ref. [44]. (rhs) The distribution in the number of charged particles for pseudo-rapidity $|\eta| < 0.3$ from PHSD for p-p, p-Pb and minimum bias Pb-Pb at the same energies as on the lhs.

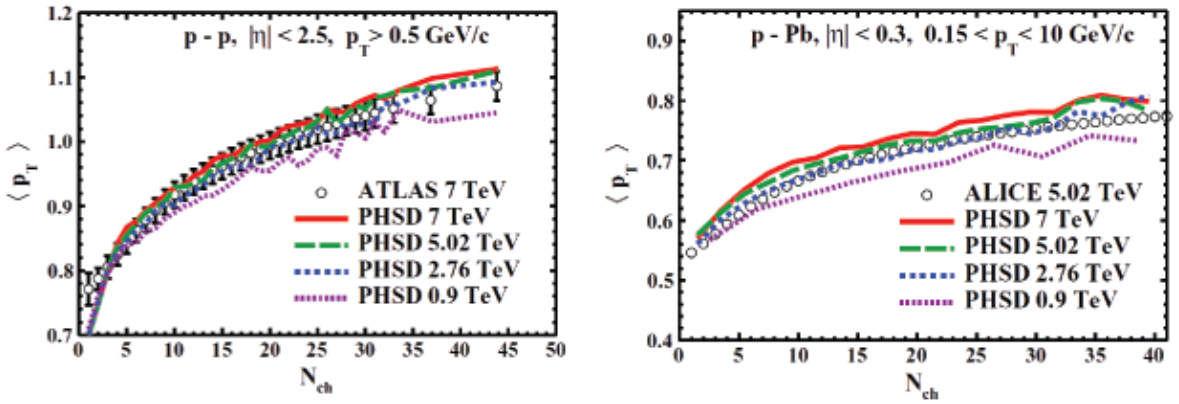


**Figure 7.** The correlation $< p_T >$ versus the number of charged hadrons at midrapidity for different bombarding energies for $p-p$ (lhs) and $p-Pb$ collisions (rhs) from 0.9 to 7 TeV. Note the different pseudo-rapidity and transverse momentum cuts!

*2.4. Correlations between the transverse momentum and the number of charged particles at midrapidity*

As a next step we will look for correlations and see how they evolve from p-p to p-Pb and Pb-Pb collisions. In Fig. 6 (lhs) we compare the average $< p_T >$ as a function of charged particle multiplicity $N_{ch}$ in p-p reactions at $\sqrt{s_{NN}} = 7$ TeV, p-Pb collisions at $\sqrt{s_{NN}} = 5.02$ TeV and Pb-Pb collisions at $\sqrt{s_{NN}} = 2.76$ TeV from the PHSD to the experimental data from Ref. [44]. Note that for low multiplicities ($N_{ch} < 5$) the mean $p_T$ is almost independent on the energy and the system (see also Ref. [44]) which in PHSD can be traced back to the fact that (for the acceptance $|\eta| \leq 0.3$, $0.15 \leq p_T \leq 10$ GeV/c) only events with one or two binary collisions $N_{bin}$ are selected for all systems. However, with increasing number of charged particles $N_{ch}$ the $< p_T >$ evolves quite differently for p-p, p-Pb and Pb-Pb collisions which was hard to get in

traditional approaches. Note, however, that the distribution in the charged particle multiplicity is very different for p-p, p-Pb and minimum bias Pb-Pb collisions (rhs). This shows that only very peripheral Pb-Pb collisions may contribute to the correlation shown in Fig. 6 (lhs) with a low number of binary collisions.

At first sight one might attribute the very different correlations to the lower bombarding energies for p-Pb and Pb-Pb collision, however, this does not hold true since the correlation for p-p and p-Pb show practically the same (low) energy dependence as seen from the PHSD calculations in Fig. 7.

To shed further light on the question we have a look at the transverse momentum of all charged particles for p-Pb at $\sqrt{s_{NN}} = 5.02$ TeV from the PHSD approach as a function of $N_{ch}$ (for the acceptance $|\eta| \leq 0.3$, $0.15 \leq p_T \leq 10$ GeV/c) on an event-by-event basis (Fig. 8 (lhs)). Here the fluctuations in $p_T$ are large compared to the ensemble average $< p_T >$ (orange line) especially for low $N_{ch}$. Accordingly, e.g. a transverse momentum $p_T = 0.6$ GeV/c does not correlate at all with $N_{ch}$! Furthermore, in these events for p-Pb the number of hard binary collisions $N_{coll}$ varies from 1 up to numbers even above 10 (Fig. 8 (rhs)) when expecting at least one charged particle within the acceptance restricted to a very low window in pseudorapidity. For this event class the average number of hard collisions is $N_{coll} \approx 4$. We note in passing that patterns very similar to Fig. 8 (lhs) are also found for Pb-Pb collisions at $\sqrt{s_{NN}} = 2.76$ TeV.

In order to provide some global views on the reaction dynamics we display in Fig. 9 the intensity in the events (lhs) and the ensemble average $< p_T >$ (rhs) as a function of $N_{coll}$ and $N_{ch}$ from PHSD for $p - Pb$ collisions at $\sqrt{s_{NN}} = 5.02$ TeV. Whereas the average number of charged particles $< N_{ch} >$ scales linearly with the average number of hard collisions $< N_{coll} >$ (as expected) this does not hold by far for the individual events! Furthermore, the average transverse momentum $< p_T >$ for fixed $N_{coll}$ and $N_{ch}$ is roughly constant (rhs) and thus shows practically no correlations also with $N_{coll}$. Note that a fixed $N_{ch}$ (or $< p_T >$) can be obtained by reactions with a varying number of binary collisions $N_{coll}$. Each of these binary reactions (for larger $N_{coll}$) then has a low $N_{ch}$ and $< p_T >$, respectively. The ensemble averages finally lead to the average correlations shown in Fig. 6 (lhs).

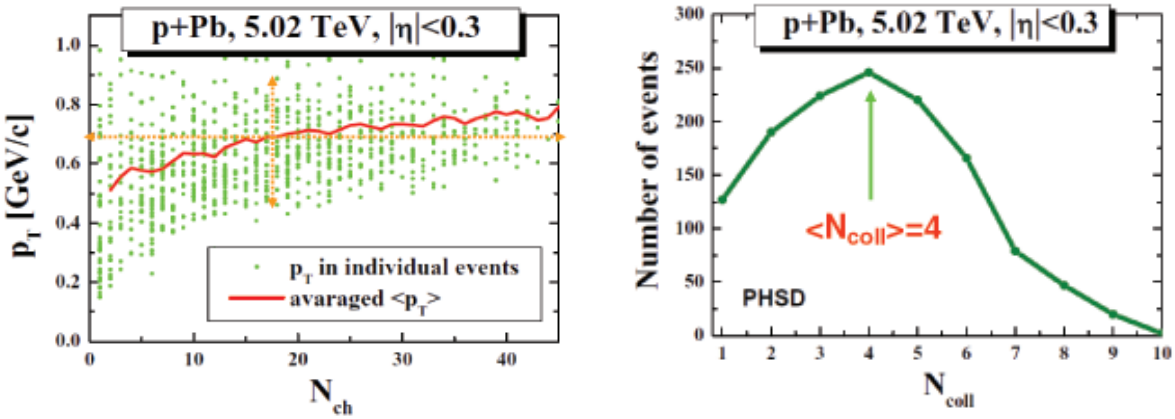


**Figure 8.** The correlation $p_T$ versus the number of charged hadrons $N_{ch}$ from PHSD for $|\eta| < 0.3$ on an event-by-event basis. The ensemble average $< p_T >$ is given by the orange solid line. (rhs) The number ofevents with at least one charged particle within the narrow acceptance as a function of the number of hard binary collisions $N_{coll}$ for $p - Pb$ collisions at $\sqrt{s_{NN}} = 5.02$ TeV.

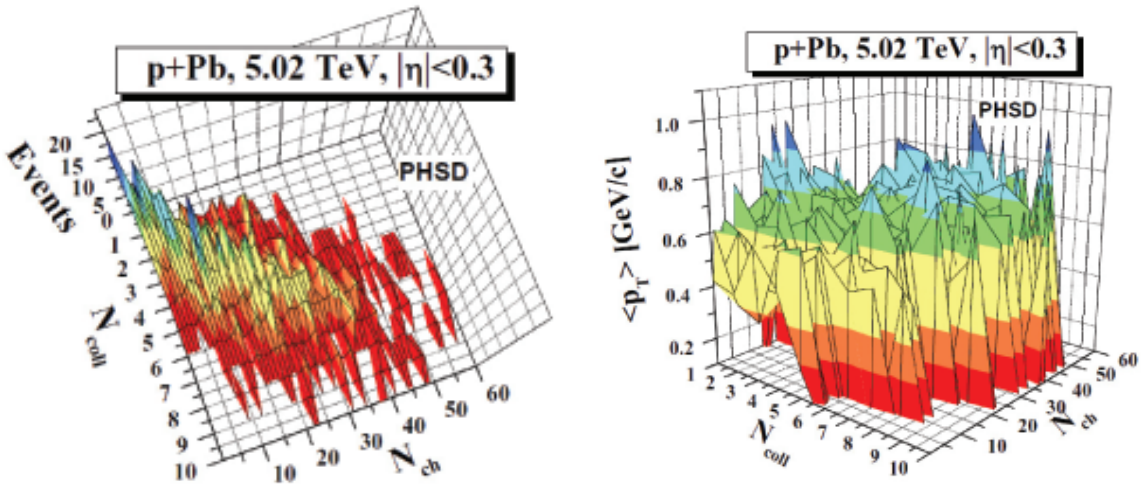


**Figure 9.** The intensity in the events (lhs) and the ensemble average $< p_T >$ (rhs) as a function of $N_{coll}$ and $N_{ch}$ from PHSD for $p - Pb$ collisions at $\sqrt{s_{NN}} = 5.02$ TeV within the acceptance ($|\eta| \leq 0.3$, $0.15 \leq p_T \leq 10$ GeV/c).

## 3. Conclusions

In this study the parton-hadron-string dynamics (PHSD) approach has been employed in the LHC energy range for Pb-Pb collisions at $\sqrt{s_{NN}} = 2.76$ TeV as well as p-Pb collisions at $\sqrt{s_{NN}} = 5.02$ TeV. We find that this approach works reasonably for both systems with respect to charged particle spectra as well as collective flow coefficients $v_2, v_3$, $v_4$ and $v_5$ for different centralities with a quality comparable to that achieved at RHIC energies before [20, 27, 28, 29, 40, 41]. Our finding implies that the 'soft' physics in Pb-Pb collisions at the LHC and Au-Au interactions at the top RHIC energies – despite a factor of $\sim 14$ in $\sqrt{s_{NN}}$ – is very similar and in line with the dynamical quasiparticle model (DQPM) that defines the parton properties for PHSD in equilibrium. This finding is common with earlier studies using viscous hydro approaches with varying initial conditions [9]. In Pb-Pb collisions the PHSD calculations have shown no sensitivity on the initial size of spatial fluctuations for the flow harmonics $v_2$ to $v_4$ which on one hand can be traced back to the low interaction rate in the initial nonequilibrium stage in PHSD ($\sim 0.3$ fm/c) where effects from different granularities are already washed out to some extent. This is different from hydro calculations with varying granularity that instantly start to convert fluctuations in coordinate space to collective modes in momentum space. On the other hand our method for changing the size of initial fluctuations keeps the event shape in coordinate space approximately invariant (cf. [42]) which - in line with hydrodynamics - leads to very similar flow coefficients $v_n$. We mention that the low interaction rate in this very early phase in PHSD is common with the CGC concept and thus does not allow to disentangle or determine the effective degrees-of-freedom in this 'pre-hydro' phase.

Furthermore, we have examined in more detail the correlations in the average transverse momentum $< p_T >$ versus the number of charged particles $N_{ch}$ at midrapidity for p-p, p-Pb and minimum bias Pb-Pb events as measured by the ALICE Collaboration in Ref. [44] at different LHC energies. The reasonable reproduction of the data within PHSD could be traced back to the large fluctuations in the number of binary collisions $N_{coll}$ for a fixed number of charged particles $N_{ch}$ as well as huge fluctuations in $p_T$ for fixed $N_{ch}$ (on an event-by-event basis). Furthermore, the individual average $< p_T >$ only weakly correlates with $N_{coll}$ and the number of charged particles $N_{ch}$ within the narrow acceptance $|\eta| < 0.3$.

**Acknowledgments**
This work in part was supported by the LOEWE center HIC for FAIR as well as by BMBF.

## 4. References

[1] Ollitrault J Y 1992 *Phys. Rev.* D **46** 229
[2] Heinz U and Kolb P 2002 *Nucl. Phys.* A **702** 269
[3] Shuryak E V 2009 *Prog. Part. Nucl. Phys.* **62** 48
[4] Shuryak E V 2005 *Nucl. Phys.* A **750** 64
[5] Gyulassy M and McLerran L 2005 *Nucl. Phys.* A **750** 30
[6] Cheng M *et al.* 2008 *Phys. Rev.* D **77** 014511
[7] Aoki Y *et al.* 2009 *JHEP* **0906** 088
[8] Schenke B Tribedy P and Venugopalan R 2012 *Phys. Rev.* **C 86** 034908
[9] Gale C Jeon S Schenke B Tribedy P and Venugopalan R 2013 *Phys. Rev. Lett.* **110** 012302
[10] McLerran L 2007 *Nucl. Phys.* A **787** 1
McLerran L 2007 *Int. J. Mod. Phys.* A **21** 694
[11] Dumitru A Kharzeev D E Levin E M and Nara Y 2012 *Phys. Rev.* C **85** 044920
[12] Tribedy P and Venugopalan R 2012 *Phys. Lett.* B **710** 125
[13] Albacete J L Dumitru A Fujii A and Nara Y 2013 *Nucl. Phys.* A **897** 1
[14] Andrs C Moscoso A and Pajares C 2014 *Phys. Rev. C* **90** 054902
[15] Bzdak A and Skokov V 2013 *Phys. Rev. Lett.* **111** 182301
[16] Nonaka C and Bass S A 2007 *Phys. Rev.* C **75** 014902
[17] Qin G-Y Petersen H Bass S A and Müller B 2010 *Phys. Rev.* C **82** 064903
[18] Plumari S Puglisi A Scardina F and Greco V 2012 *Phys. Rev.* C **86** 054902
[19] Xu Z and Greiner C 2005 *Phys. Rev.* C **71** 064901
[20] Cassing W and Bratkovskaya E L 2009 *Nucl. Phys.* A **831** 215
Bratkovskaya E L *et al.* 2011 *Nucl. Phys.* A **856** 162
[21] Abelev B *et al.* [ALICE Collaboration] 2013 *Phys. Rev. Lett.* **110** 032301
[22] Barnafoldi G G Barrette J Gyulassy M Levai P and Topor Pop V 2012 *Phys. Rev.* C **85** 024903
[23] Xu R Deng W-T and Wang X-N 2012 *Phys. Rev.* C **86** 051901
[24] Juchem S Cassing W and Greiner C 2004 *Nucl. Phys.* A **743** 92
[25] Cassing W 2009 *E. Phys. J. ST* **168** 3
[26] Cassing W and Bratkovskaya E L 1999 *Phys. Rept.* **308** 65
Cassing W Bratkovskaya E L and Juchem S 2000 *Nucl. Phys.* A **674** 249
Bratkovskaya E L and Cassing W 1997 *Nucl. Phys.* A **619** 413
Geiss J Cassing W and Greiner C 1998 *Nucl. Phys.* A **644** 107
[27] Toneev V D *et al.* 2012 *Phys. Rev.* C **85** 034910
[28] Konchakovski V P Bratkovskaya E L Cassing W Toneev V D and Voronyuk V 2012 *Phys. Rev.* C **85** 011902
[29] Linnyk O Cassing W Manninen J Bratkovskaya E L and Ko C M 2012 *Phys. Rev.* C **85** 024910
Linnyk O Bratkovskaya E L Ozvenchuk V Cassing W and Ko C M 2012 *Phys. Rev.* C **84** 054917
[30] Linnyk O *et al.* 2013 *Phys. Rev.* **C 87** 014905
[31] Sjostrand T Mrenna S and Skands P Z 2006 *JHEP* **0605** 026
[32] Bengtsson H-U and Sjöstrand T 1987 *Comp. Phys. Commun.* **46** 43
[33] Aad G *et al.* [ATLAS Collaboration] 2011 *New J. Phys.* **13** 053033
[34] Konchakovski V P Cassing W and Toneev V D 2014 *J. Phys.* G **41** 105004
[35] Balitsky I 1996 *Nucl. Phys.* B **463** 99
Kovchegov Y V 1999 *Phys. Rev.* D **60** 034008
[36] Gelis F Iancu E Jalilian-Marian J and Venugopalan R, *Ann. Rev. Nucl. Part. Science* **60** 463
[37] ATLAS collaboration, ATLAS-CONF-2013-096
[38] Abelev B B *et al.* [ALICE Collaboration] 2014 *Phys. Lett.* B **736** 196
[39] Aamodt K *et al.* [ALICE Collaboration] 2011 *Phys. Rev. Lett.* **107** 032301
[40] Linnyk O Cassing W and Bratkovskaya E L 2014 *Phys.Rev.* C **89** 034908
Linnyk O Konchakovski V P Cassing W and Bratkovskaya E L 2013 *Phys. Rev.* C **88** 034904
[41] Konchakovski V P *et al.* 2012 *Phys. Rev.* C **85** 044922
[42] Konchakovski V P Cassing W and Toneev V D 2015 *J. Phys. G* **42** 055106
[43] Bilandzic A Snellings R and Voloshin S 2001 *Phys. Rev.* C **83** 044913
[44] Abelev B B *et al.* [ALICE Collaboration] 2013 *Phys. Lett.* B **727** 371